

Temperature Sensor for Hydro Generator Bearings using Thermally Regenerated Fiber Bragg Gratings

Uilian José Dreyer, Kleiton de Morais Sousa,
 Cicero Martelli, Valmir de Oliveira,
 Hypolito J. Kalinowski, Jean Carlos Cardozo da Silva
 Graduate Program in Electrical and Computer Engineering
 Federal University of Technology - Paraná (UTFPR)
 Curitiba, Brazil
 Email: jeanccs@utfpr.edu.br

Erlon Vagner da Silva
 Maintenance Department
 Tractebel Energia, UHE Salto Osório
 Quedas do Iguaçu, Brazil
 Email: erlon@tractebelenergia.com.br

Abstract—This work presents the design and experimental results of a temperature sensor based on quasi-distributed thermally regenerated Fiber Bragg gratings (RFBG) applied to the bearings of hydro generators. The temperature increase in the bearing is generally due to excessive shaft misalignment, low oil level or dirt in the lubricant oil. Expensive and time-consuming damage can be caused to the generator if the temperature sensors are not able to detect the fault in time and accurately. The proposed sensor has three wavelength multiplexed RFBG to monitor the vertical temperature gradient in the lubricant oil. The developed package is designed to avoid the cross sensitivity of the RFBG with mechanical forces. Thermally treated Fiber Bragg Grating (FBG) is heated till about 900 °C far away the temperature range in which the power plant operates, making its use suitable to obtain thermal stability for many years. Temperature stability tests were carried out for over fourteen hours in laboratory. The uncertainties were evaluated considering the sample dispersion and equipment characteristics used during the sensor temperature calibration. The experimental results show that the uncertainty associated to each FBG matches the power plant metrological requirements. The developed package for bearing temperature measurement proved to be robust both mechanically and thermally.

Keywords—*Electrical generator bearing; Optical Regenerated Fiber Bragg Gratings; Temperature measurement.*

I. INTRODUCTION

The Brazilian energy sector is predominantly hydroelectric which represents approximately 62 % of the total energy generated in the country. The installed electrical energy capacity reaches 90.2 GW in a total of 145.5 GW, meaning about five times the capacity of thermal power plants that use natural gas fuel, which is the second largest Brazilian electrical energy source with about 18.1 % of the total [1]. The electric generators used in large power plants have sizes normally reaching hundreds of Mega Watts (MW). They have also heavy structures with dimensions proportional to its power causing the cooling and alignment systems to be an important part of these large machines.

Therefore, hydroelectric power plants must operate uninterrupted for long periods of time before a preventive maintenance of the generation system is required. The electrical generator has a very important role in the generation system because of it is the machine that converts the mechanical

energy coming from the hydraulic turbine into electric energy. However, power generators are susceptible to adverse situations such as unbalanced loads, short-circuits in the transmission line among others. These situations cause, mainly, a higher loss in the windings of the generator (stator and rotor) and therefore a temperature rise above the expected and planned for its operation. When the temperature is above the nominal it causes premature wear of the insulating materials reducing the service life of the generator [2].

In Figure 1, there is a schematic drawing showing the bearings position along the hydro generator structure. The bearing indicated by 1 is the one that supports the vertical force exerted by the weight of the hydraulic turbine (HT) and electrical generator (EG) assembly. The bearings indicated by 2 and 3 are intended to not allowing the misalignment of hydro generator in the horizontal direction. The EG is a three-phase synchronous generator, with a rated voltage of 13.8 kV between phases, and rated current of 7.1 kA. The generator stator has a diameter of 12 m and 2.5 m in height. The structure weighs over 200 tons implying serious safety problems if any alignment issue takes place. With a reliable system to monitor temperature continuously, small temperature increases can be detected before causing further damage.

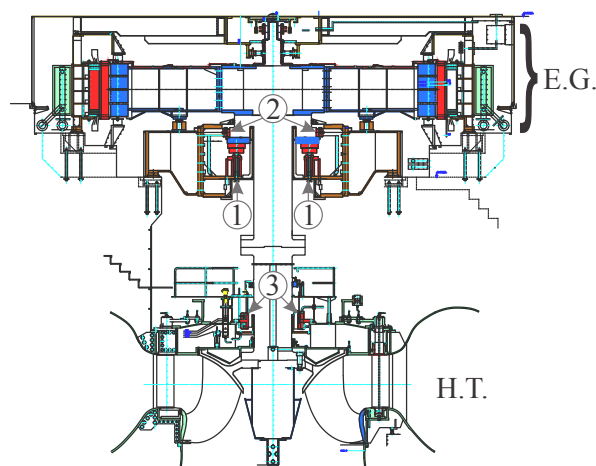


Figure 1. Drawing showing the bearing positions into a 200 MVA hydro generator installed in Salto Osório power plant.

Apart from thermal induced drawbacks, mechanical align-

ment also can lead to faults in the large hydroelectric power generators. The bearings must compensate potential misalignment in the shaft that connects the hydraulic turbine to the generator. The torsional efforts coming from different power cycles that the generator is subject to must also be compensated [3][4]. When the generator operates by varying its power, there is a proportional temperature variation on the bearings, therefore increasing their temperature with the increase in the generated power. There are other factors like lack of lubrication or dirty contaminants in lubricant reservoir, which increase temperature, sometimes leading to the generator shutdown and the necessity to perform corrective maintenance. In Figure 2, it is presented a damaged bearing by metal pieces that fell into the lubricant oil causing the generator shutdown by temperature increase. Another important factor that could affect the bearings temperature is the short-circuit stator winding which induces abnormal electromagnetic flux in the air gap, and, as a result, the excessive vibrational movements in the generator-turbine shaft [5].



Figure 2. Photography of a damaged bearing that is disassembled to perform corrective maintenance.

In this work, we present the development and results of an optical fiber sensor developed to monitor bearings in hydro generator that avoid FBG cross-sensitivity [6]. The proposed design uses three wavelength multiplexed and encapsulated Regenerated Fiber Bragg grating sensors (RFBG) that form a thermal transducer of 1.5 m long and has sensing points distributed along its body. The FBG has some promising features that make it wide applicable in electric machines [7][8]. A FBG sensor [9] consists of an optical fiber passive-device that have shown fast insertion in measuring and control applications. The FBG led to new developments in optical filtering and in the design of sensors. FBG temperature sensors have some advantageous characteristics, such as low mass, immunity to electromagnetic interference, small signal attenuation and the possibility of being multiplexed [10]. Thus, it has the ability to solve measurement issues for which conventional sensing techniques are not appropriate, as in the case of the thermal analysis inside large electric generators working at high voltages.

The next sections provide a more specific approach to the main issues related to the developed optical fiber sensor. A brief review about FBG and RFBG is presented in Section II highlighting this main characteristics. In Section III it is presented the packaging assembly, the temperature calibration process and the method used to determine uncertainties. The experimental results are presented in Section IV. Finally, the conclusions obtained from the temperature tests and future work are presented in Section V.

II. THERMALLY REGENERATED FIBER BRAGG GRATINGS

An FBG is formed by a periodic change in the refractive index caused in a fiber core with an effective refractive index n_{eff} by exposure to an ultraviolet (UV) laser beam [6]. The index change is perpendicular to the longitudinal axis of the fiber with constant periodicity Λ . The index modulation inside the fiber builds a resonant structure to a determinate wavelength as shown in Figure 3. The center peak wavelength is called Bragg wavelength (λ_B) and is given by (1):

$$\lambda_B = 2n_{eff}\Lambda. \quad (1)$$

Figure 3 (a) shows an optical fiber in which three FBGs are inscribed with different modulation period Λ . The different periods lead to different resonances Bragg wavelength λ_B . When the Bragg condition is satisfied (1), the light reflected back by each modulation contributes constructively. Then a central wavelength of the reflected light is defined by the parameters of the grating [13]. The reflected spectrum (S_r) is similar to a very effective band-pass filter and the transmitted spectrum (S_t) resembles a reject-band filter as shown in Figure 3 (b).

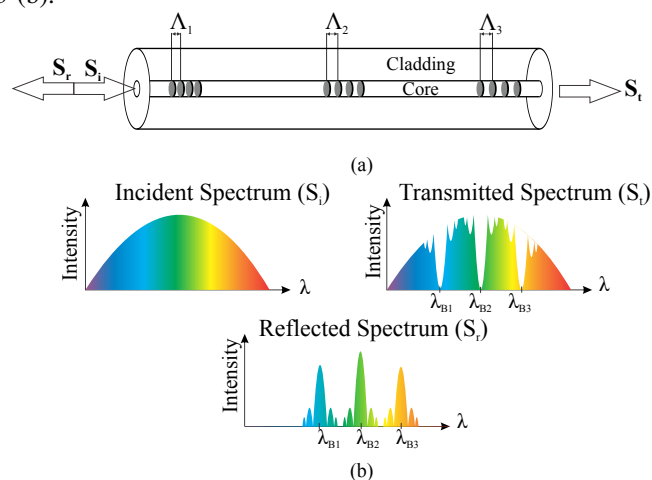


Figure 3. Schematic representations of three wavelength multiplexed FBGs inscribed into an optical fiber (a) and its associated spectra (b).

The Bragg wavelength (λ_B) has dependency on two parameters: effective refractive index and grating periodicity. The change on one of these two parameters from external interference produces a shift in λ_B . The mechanical and thermal environment changes are related to the wavelength shift through the expression:

$$\Delta\lambda_B(l, T) = 2 \left(\Lambda \frac{\partial n_{eff}}{\partial l} + n_{eff} \frac{\partial \Lambda}{\partial l} \right) \Delta l + 2 \left(\Lambda \frac{\partial n_{eff}}{\partial T} + n_{eff} \frac{\partial \Lambda}{\partial T} \right) \Delta T. \quad (2)$$

The first term in (2) represents the strain effect on an optical fiber. It is associated with the shift on λ_B due to the change of the refractive index, called photo-elastic coefficient, and the length of the FBG caused by the optical fiber mechanical deformation. As for the second term in (2), λ_B shift is associated with the thermal expansion coefficient and the thermo-optic coefficient of silica. The influence of the thermo-optic coefficient surpasses by far the thermal expansion coefficient in a silica optical fiber. It is also possible to observe that the FBG has a cross sensitivity between strain and temperature. So, when it is desired to build a temperature sensor it is necessary to develop a package that eliminates the strain effect.

There is a concern to improve the thermal properties of FBG to allow temperature sensing applications with improved the temperature stability of the gratings. This has involved experimenting with various dopants, including Sn and Na₂O [14]. Previous studies have already established that temperature range and stability of FBGs can be improved by several means, including formation of type IIA [15][16][17] and type II [18][19] gratings, including those inscribed using femtosecond IR lasers.

For many applications, the thermal stability of laser induced glass changes determines the limits in which they can operate, for power plant applications, FBGs that can operate at 80 °C for 25 years are required. Thermally regenerated FBG play a special role in temperature measurement inside power plants because of it has great thermal stability within the power plant temperature range [11][12]. In order to make a RFBG, it is inscribed a strong conventional Bragg grating into hydrogen loaded optical fiber called seed grating. Afterwards, the strong seed grating is thermally processed at about 900 °C and the regeneration is observed. Over time as the seed grating disappears completely, a regenerated grating appears [20][21].

The temperature sensing in hydroelectric generators has a great importance as a performance indicator of the machine, and it is frequently measured using RTD or thermocouples as point sensors. Although widely used, such sensors can easily be interchange by new technologies like optical fiber sensors, especially those designed with FBG, as presented in this work. Optical fiber sensing applications in hydro generators were presented in [22][23] demonstrating the monitoring of temperature, vibration, magnetic field among others generator parameters. There is also the use of distributed temperature sensing on the stator surface of 200 MVA generator [24]. Furthermore, the temperature monitoring in bearings using FBG was developed and tested in laboratory during 12 hours [25].

III. PACKAGING AND TEMPERATURE CALIBRATION

The seed FBGs used in this work were produced at the Photonics Laboratory of UTFPR, using ArF Excimer lasers (Coherent Xantos) operating at 193 nm. The gratings were directly written using a phase-mask with typical laser pulse energy of 5 mJ and repetition rate of 250 Hz, with exposition on the order of 5 minutes. Each grating has approximately 3 mm in length.

The fiber samples are hydrogen loaded for several days under 110 atm, 25 °C before the seed grating inscription. The grating was kept at room temperature after inscription to diffuse hydrogen before being subjected to the regeneration process inside a resistive oven. Using a processing procedure identical to [26], strong seed gratings were thermally processed with temperatures between 21 °C to 900 °C (± 15 °C) during approximately 2 h 30 min. At 900 °C the regeneration is observed, and over time as the seed grating is reduced almost completely, the regenerated grating appears. After that, the oven is turned off and the grating remained resting inside to complete the annealing process. Figure 4 shows the spectrum of the seed FBG (dashed line) and RFBG (solid line) after the annealing process.

Due to the harsh environment and the fragility of pristine FBG sensors, the FBG must be packaged with special materials

before installation, to avoid the damage to the fiber sensors. Another feature of the package should be the minimization of the strain-temperature cross sensitive of FBG. In this work the package is formed by one steel rod with an external diameter of 3.18 mm and an internal hole with a diameter of 1.7 mm. Fig 5 (a) and (b) show pictures of the sensor package for bearing sensor.

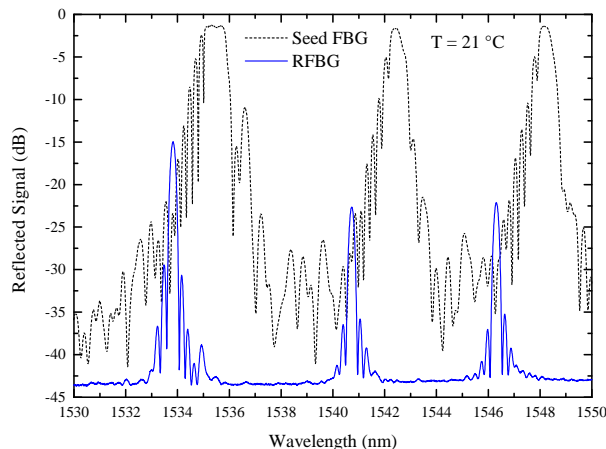


Figure 4. Spectrum of the seed FBG (dashed line) and regenerated FBG (solid line) after the thermal treatment.

In Figure 5 (a), there is a drawing showing the main sensor parts. The sensor presents a splice chamber to keep the optical splices safe and an optical cable exit to connect the RFBGs to the internal optical aqua plant link. The junction applies a force to the collet, it causes a pressure to hold the steel rod on the sensor and inside the thermowell. The bearing sensor has three RFBGs spatially positioned close to it edges (Figure 5 (b)). This distributed sensor configuration was designed because of the three FBG will be immersed in the oil to detect the temperature gradient along the vertical direction.

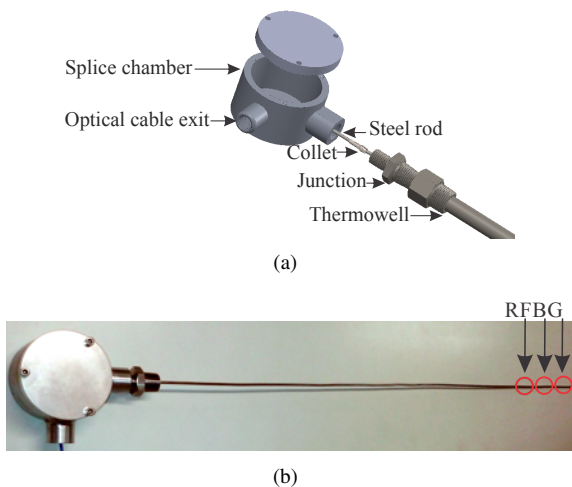


Figure 5. Optical fiber sensor assembly (a) mechanical modeling and (b) photo.

The calibration system and process are based on the diagram presented in Figure 6 (a). The optical fiber sensor (OFS) and the Platinum Resistance thermometer (PT100) sensor are placed inside a copper tube in which water is pumped through it using the thermal bath flow (TB). While the flow is maintained, a digital multimeter (DM) and the optical

interrogator (OI) measure the PT100 and the Bragg gratings, respectively. These are all connected/controlled by a home made software implemented in LabVIEWTM, that automate the calibration process as well as the uncertainty calculations [27].

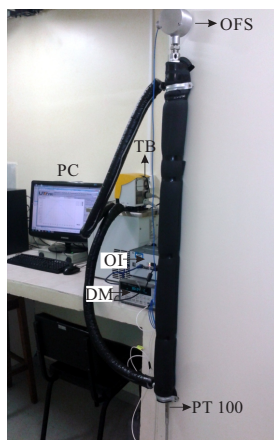
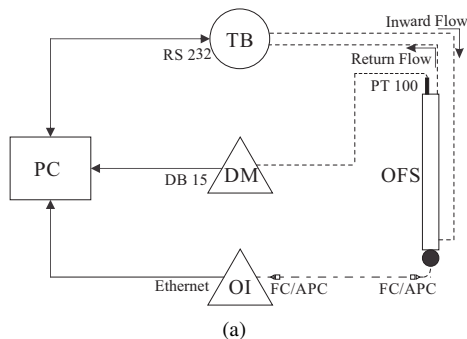


Figure 6. Designed calibration system (a) function diagram and (b) assembly photo.

The measurement uncertainty usually encompasses many requisites. Some can be estimated through a type A evaluation of measurement uncertainty from the statistical distribution values. The values come from several measurements and can be characterized by standard deviations. Other components can be estimated through a type B evaluation of measurement uncertainty. They may also be characterized by standard deviations estimated from probability density functions based on user experience or other information [28][29]. The A and B type uncertainties followed the diagram shown in Figure 7 to this particular sensor.

The calibration process consisted of heating cycles repeated four times, from 10 °C to 80 °C for the optical fiber sensor. The largest uncertainty associated with each sensor is presented in Table I. With the temperature calibration points, a corresponding function is shown to represent the FBG temperature (T) response with its Bragg wavelength as showed in Figure 8 to each RFBG. In this case, a second order polynomial function in (3) is fitted with the α (second order) and β (first order) coefficients presented in the Table I, while the constant coefficient γ , which is characteristic for each grating resonance Bragg wavelength (λ):

$$T(\lambda) = \alpha\lambda^2 + \beta\lambda + \gamma \quad (3)$$

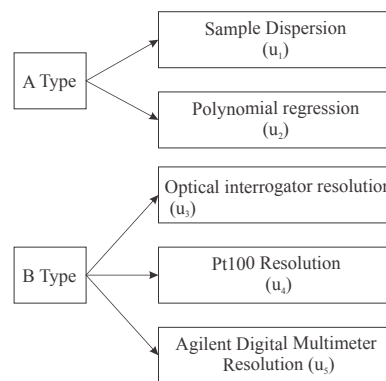


Figure 7. Diagram with parameters involved in uncertainty evaluation for this particular project.

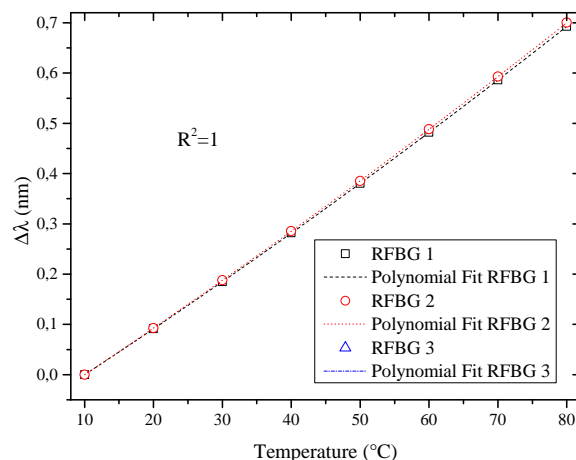


Figure 8. Figure of the polynomial fit for the temperature calibration points using the optical fiber sensor with RFBG.

Sensor	Function fit coefficients	Uncertainty
RFBG 1	$T(\lambda) = 1.3 \times 10^{-5} \lambda^2 + 8.748 \times 10^{-3} \lambda + 1536,951$	0.78 °C
RFBG 2	$T(\lambda) = 1.2 \times 10^{-5} \lambda^2 + 8.916 \times 10^{-3} \lambda + 1540,406$	0.38 °C
RFBG 3	$T(\lambda) = 1.2 \times 10^{-5} \lambda^2 + 8.886 \times 10^{-3} \lambda + 1543,405$	0.36 °C

The fitted functions, having their coefficient values presented in Table I, are approximately the same for every grating of each individual optical fiber sensor.

IV. RESULTS AND DISCUSSIONS

The same calibration system was used for testing the bearing sensor in order to apply temperature step function excitations such as to compare the FBG measurements with a PT100 used in the generator. The thermal cycles ranged from 15 °C to 75 °C, lasting for 15 hours. The thermal cycles had the goal of emulating four loading levels in the hydro generator (Figure 9): 15 °C - turned off, 35 °C - energy compensator, 55 °C - nominal charge and 75 °C - overloaded. The overload occurs at temperatures above 70 °C and the generator is turned off by the temperature system protection. In Figure 9, the ‘A’ inset indicates a steady state period during the experiment.

It is possible to observe in Figure 9 that the optical fiber Bragg grating sensor temperature measurements follow the

same trend as the PT100 sensor. A small difference is observed in the time response (inset) that can be accounted for the distinct positioning inside of the test chamber of the thermal bath. In four temperature cycles the 3 RFBGs temperature sensors measured the same value as the PT100 sensor and the small differences are smaller than the determined uncertainty for each individual sensor.

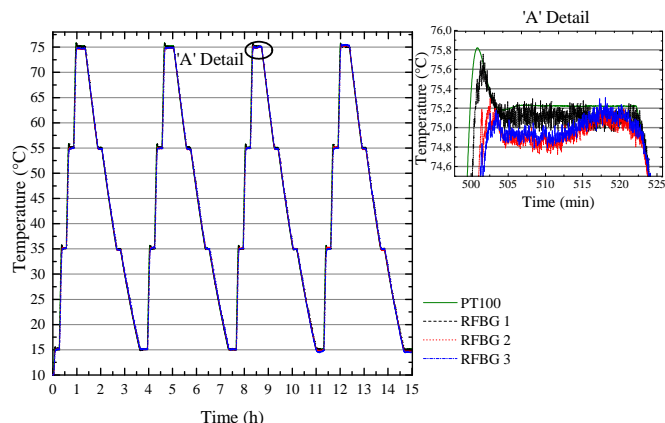


Figure 9. Laboratory essay lasting over 15 h with the 3 RFBG compared to the PT100 sensor.

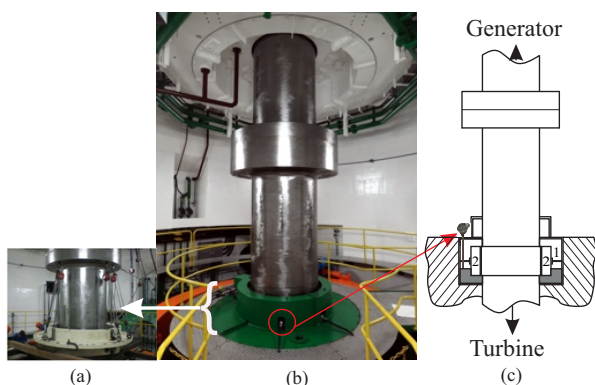


Figure 10. (a) Babbitted shoe metal pulled off from the bearing assembly to perform a maintenance procedure. (b) Bearing photography inside the power plant and (c) the schematic representing the parts that play an important role on the bearing .

The bearing where the RFBG optical fiber sensor will be installed is shown in Figure 10 (b)-(c), and the details (1) – (2) represent the lubricant oil and babbitted shoe metal, respectively, being those two points to be monitored. The lubricant oil has the role of reducing the friction between the shaft and the babbitted shoe metal, and its temperature is an indicator of the machine operation status. Figure 10 (a) also shows the babbitted shoe metal being pulled off from the bearing assembly to undertake a maintenance procedure.

V. CONCLUSION

The potential of integrating fiber Bragg grating sensors for multiplexed on-line monitoring of temperature and temperature gradients has been experimentally investigated in laboratory and inside a power plant before this presented work [25]. In general, it is noticed that the temperature is fully consistent with the actual operation of the bearing. The presented analysis can indicate the operating condition of the equipment and the results demonstrate that this technique is a potential maintenance tool for predictive purposes with a high efficiency

to continuously monitor the hydro generator facilities. The generator designers could also use these measurements to improve the machine performance and establish their limits of safe operation. Future work include temperature measurements on a bearing to measure the temperature in the turbine bearing of a hydroelectric 180 MW generator inside the power plant.

ACKNOWLEDGMENT

The authors acknowledge the financial support of ANEEL, CNPq, CAPES, FINEP, Fundação Araucária, and Tractebel Energia. This project is developed under Tractebel Energia’s R&D program (PD-0403-0028/2012), regulated by ANEEL.

REFERENCES

- [1] ANEEL, “Brazilian Electricity matrix,”. URL: www.aneel.gov.br [retrieved: 06–2015].
- [2] G. Stone, and J. Kapler, “Stator winding monitoring,” *Industry Applications Magazine*, IEEE, vol 4, 1998, pp. 15–20.
- [3] C. E. J. Bowler, P. G. Brown, and D. N. Walker, “Evaluation of the effect of power circuit breaker reclosing practices on turbine-generators shafts,” *Power Apparatus and Systems, IEEE Transactions on PAS-99*, vol. 5, 1980, pp. 1764–1779.
- [4] D. Stojanovic, D. Petrovic, and N. Mitrovic, “Torsional torques of big turbine-generator shafts due to malsynchronization,” in [Electrotechnical Conference, 2000. MELECON 2000. 10th Mediterranean], vol. 3, 2000, pp. 1051–1054.
- [5] A. Tetreault, “Rotor shape vs. rotor field pole shorted turns: Impact on rotor induced vibrations on hydrogenerators,” in [Condition Monitoring and Diagnosis (CMD), 2012 International Conference], 2012, pp. 133–136.
- [6] A. Othonos and K. Kalli, [Fiber Bragg gratings], vol. 68, 1999, pp. 4309-4341.
- [7] K. M. Sousa, A. A. Hafner, H. J. Kalinowski, and J. C. C. da Silva, “Determination of temperature dynamics and mechanical and stator losses relationships in a three-phase induction motor using fiber bragg grating sensors,” *Sensors Journal, IEEE*, vol. 12, 2012, pp. 3054–3061.
- [8] N. M. Theune, et al. “Multiplexed temperature measurement for power generators,” *Proc. SPIE*, vol. 4074, 2000, pp. 214–221.
- [9] R. Kashyap, [Fiber Bragg Gratings], Electronics & Electrical, Academic Press (1999).
- [10] T. Erdogan, “Fiber grating spectra,” *Journal of Lightwave Technology*, vol. 15, 1997, pp. 1277–1294.
- [11] J. Canning, S. Bandyopadhyay, M. Stevenson, and K. Cook, “Ultra-High Temperature (UHT) Gratings,” vol. no , 2008, pp. 1–3 (2008).
- [12] J. Canning, et al., “Regenerated gratings,” *Journal of the European Optical Society - Rapid publications*, vol. 4, 2009, ISSN 1990-2573.
- [13] K. O. Hill and G. Meltz, “Fiber Bragg grating technology fundamentals and overview,” *Journal of Lightwave Technology*, vol. 15, 1997, pp. 1263–1276.
- [14] G. Brambilla and P. Hua, “Phase separation in highly photosensitive tin-codoped silica optical fibers and fiber preforms exposed to {UV} radiation,” *Journal of Non-Crystalline Solids*, vol. 352, 2006, pp. 2921 – 2924.
- [15] I. Riant and F. Haller, “Study of the photosensitivity at 193 nm and comparison with photosensitivity at 240 nm influence of fiber tension: type IIa aging,” *Journal of Lightwave Technology*, vol. 15, 1997, pp. 1464–1469.
- [16] O. Prakash, et al., “Enhanced temperature 800 °c stability of type-ii-a fbg written by 255 nm beam,” *Photonics Technology Letters, IEEE*, vol. 26, 2014, pp. 93–95.
- [17] E. Lindner, et al., “Thermal regenerated type {IIa} fiber bragg gratings for ultra-high temperature operation,” *Optics Communications*, vol. 284, 2011, pp. 183 – 185.
- [18] H. Y. Liu, H. B. Liu, G. D. Peng, and P. L. Chu, “Observation of type i and type {II} gratings behavior in polymer optical fiber,” *Optics Communications*, vol. 220, 2003, pp. 337 – 343.

- [19] D. Grobnc, S. J. Mihailov, J. Ballato, and P. D. Dragic, "Type i and ii bragg gratings made with infrared femtosecond radiation in high and low alumina content aluminosilicate optical fibers," *Optica*, vol. 2, 2015, pp. 313–322.
- [20] J. Canning, M. Stevenson, S. Bandyopadhyay, and K. Cook, "Extreme Silica Optical Fibre Gratings," *Sensors*, vol.8, 2008, pp. 6448–6452.
- [21] B. Zhang and M. Kahrizi, "High-temperature resistance fiber bragg grating temperature sensor fabrication," *Sensors Journal, IEEE*, vol. 7, 2007, pp. 586–591.
- [22] M. Willsch, "Fiber Optical Sensors in Power Generation," in [Third Asia Pacific Optical Sensors Conference], vol. 8351, 2012, pp. 835137–1–835137–9.
- [23] C. Martelli, et al., "Temperature sensing in a 175MW power generator," in [OFS2012 22nd International Conference on Optical Fiber Sensors], *Proc. SPIE*, vol. 8421, 2012, pp. 84212F–1–84212F–4.
- [24] F. Mezzadri, C. Martelli, E. V. Silva, J. P. Bazzo, and J. C. C. Silva, "175MW Hydroelectric Generator Stator Surface Temperature Monitoring using a DTS System," *IEEE Sensors Journal*, vol. no , 2014, pp. JM5A.64.
- [25] E. V. da Silva, et. al., "Optical fiber instrumentation of a high power generator and turbine," *European*, vol. 8794, 2013, pp. 879446–1–879446–6.
- [26] V. Oliveira and H. J. Kalinowski, "Strongly regenerated Bragg gratings in standard single-mode fibres," *Methodology*, vol. 7653, 2010, pp. 765312–765316.
- [27] S. G. Rabinovich, "Measurement errors and uncertainties," third edition, 2005.
- [28] B. N. Taylor, and C. E. Kuyatt, "Guidelines for Evaluating and Expressing the Uncertainty of NIST Measurement Results," Technical note 1297, 1994.
- [29] A. C. Baratto, et al., "Evaluation of measurement data – Guide to the expression of uncertainty in measurement", 2008.